Hindawi
Journal of Nanomaterials
Volume 2019, Article ID 2970819, 9 pages
https://doi.org/10.1155/2019/2970819

Research Article

Influence of Varied Fluorine Contents on Long-Term Storage Stability of Polyacrylate Nanoparticles and Film Properties

Hongzhu Liu,[1] **Gaofan Zhang**,[2] **Lulu Lu**,[3] **Yuexing Chen**,[4] **Mengting Luo**,[4] **Jiming Bian**,[5] **Zefeng Wang**,[4,6] **and Lijin Wang**[4]

[1]*School of Textile and Material Engineering, Dalian Polytechnic University, Dalian 116034, China*
[2]*Wenzhou Institute, University of Chinese Academy of Sciences (Wenzhou Institute of Biomaterials & Engineering), Wenzhou 325001, China*
[3]*School of Biological Science and Engineering, South China University of Technology, Guangzhou 510640, China*
[4]*Department of Chemistry, Lishui University, Lishui 323000, China*
[5]*Key Laboratory of Materials Modification by Laser, Ion and Electron Beams (Ministry of Education), School of Physics, Dalian University of Technology, Dalian 116024, China*
[6]*Post-Doctoral Research Station, Dalian Zhenbang Fluorocarbon Paint Stock Co., Ltd., Dalian 116036, China*

Correspondence should be addressed to Zefeng Wang; shangk72@163.com and Lijin Wang; lsxywlj@lsu.edu.cn

Received 24 May 2019; Revised 9 September 2019; Accepted 27 September 2019; Published 31 October 2019

Academic Editor: Ashok K. Sundramoorthy

Polyacrylate nanoparticles are widely applied and typically prepared by many polymerization methods. However, poor long-term storage stability of nanoparticles limited their use, so some methods are carried out to overcome it. In this paper, we investigated a series of fluorinated polyacrylate nanoparticles to improve the long-term storage stability of polyacrylate nanoparticles. We found that increasing fluorine content resists the aggregation of nanoparticles during long-term storage. Furthermore, a higher content of fluorine can improve the hydrophobicity of latex polyacrylate film and increase the refractive index of latex polyacrylate film. The properties of the polyacrylate nanoparticles and latex film can thus be controlled by changing fluorine contents, which in turn provides key insights into the design of functional polymer material.

1. Introduction

Polymeric nanoparticles have attracted great interest in both academic and industrial fields owing to their potential applications in drug delivery [1–3], separation sciences [4, 5], catalysis [6, 7], diagnostic imaging [8, 9], soil remediation [10], and so on. Over the past decade, a variety of polymeric nanoparticles have been reported in the literature, including polyolefins [11], polyesters [12], polyurethanes [13], polyaryletherketones [14], polysaccharide [15], and polyacrylates [16] as well as their copolymers [16]. Polymeric nanoparticles and their films possess prominent economic value, which are applied for finishing agent [17, 18], anticorrosion coating [19], photoresponsive material [20], dielectrics, and adhesives [21].

Among them, polyacrylate nanoparticles obtained by addition polymerization of vinyl groups with the molecular structure of monomer have received much attention due to good film-forming property [16], low cost [22], controllable size [22], low toxicity [23], and ease of synthesis [16]. Various methods have been used to fabricate polyacrylate nanoparticles, such as the epitope polymerization technique [24], the supramolecular self-assembly approach [25], and the spray drying method [26]. Comparatively, the emulsion polymerization is more economical, environment-friendly, and simple [27].

On the other hand, the major barrier encountered in the application of polymeric nanoparticles is that the nanoparticles are liable to aggregation, creaming [28], and flocculate [29] due to phase separation during long-term storage. For

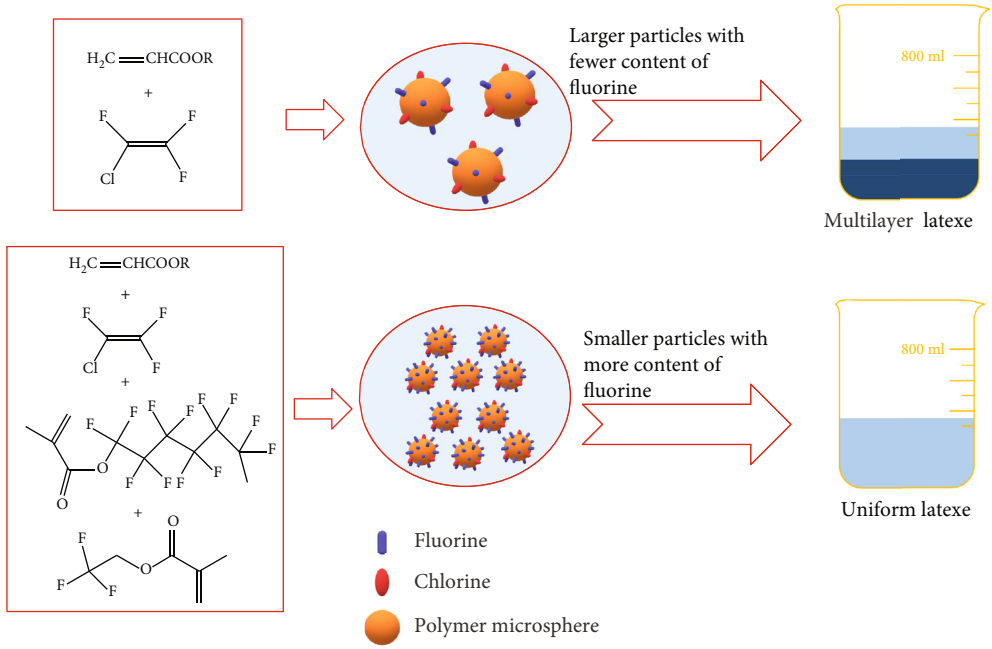

Scheme 1: Schematic illustration for the preparation of different fluorinated polyacrylate latexes.

example, it is interesting in our previous work that polymeric nanoparticles using chlorotrifluor ethylene as amphiphilicity monomer is instable in emulsion. To solve this problem, Binks and Whitby fabricated stable polymeric nanoparticles by changing the wettability of particle surface [30]. Lazzari and coworkers reported it was necessary to lower the zeta potential value of the nanoparticles in order to improve the stability of nanoparticles [31]. The work by Lemoine et al. showed that molecular weight and crystallinity of the polymer, nanoparticle size, and pH of solvent affect the stability of nanoparticles [32].

The reported results reveal that the modification of latex is an accessible method to improve the stability of nanoparticles. Logie and coworkers fabricated stable polymeric micelles by modifying hydrophilic poly(ethylene glycol) moieties [33]. Yang et al. reported the use of maleic reactive surfactants and acrylate monomers to form soap-free latex. They found that acrylate latex could stabilize against electrolyte [34]. However, to the authors' knowledge, few works about polymeric nanoparticles modified chemically by hydrophobic fluorinated groups to improve stability have been reported.

Fluorinated polymers present a great deal of interesting properties, owing to the unique features of fluorine atom. These materials are well-known in many applications, such as drug delivery [35], coatings [36], and electrolyte [37]. In order to further utilize many unique advantages conferred by the fluorinated group, the synthesis of copolymers, in which more fluorinated groups are incorporated, is essential. For instance, the polymeric materials containing more fluorine content have lower refractive index. This is conducive to the application of optical devices.

With the above considerations in mind, herein, a series of fluorinated polyacrylate latexes were synthesized by semicontinuous emulsion polymerization. As shown in Scheme 1, the introduction of high concentration of fluorine groups can effectively enhance long-term storage stability of emulsion. All latex particles contain chlorotrifluoroethylene (CTFE) monomer which is used as the research template, because we found that fluorine was only provided by CTFE and the long-term stability of latex particles is poor in the previous study [38]. Moreover, fluoroacrylate monomers can be introduced into latex particles by free radical copolymerization in a relatively simple method without complex chemical modification. In addition, since fluorinated acrylate monomers are difficult to emulsify, few reports have shown the copolymerization of CTFE with fluoroacrylate to prepare fluorinated polyacrylate latexes by emulsion polymerization. But this method is conducive to large-scale application. The chemical structure, size, and size distribution of resultant particles were investigated by FTIR and dynamic light scatterings (DLS). The wettability, thermal stabilities, and refractive index of the latex films were investigated by measurements of water contact angle, thermal gravimetric analysis (TGA), and spectroscopic ellipsometry, respectively.

2. Materials and Methods

2.1. Materials. Chlorotrifluoroethylene (CTFE), vinyl acetate (VAc), butyl acrylate (BA), and versatic acid 10 esters (Veova10) were purchased from Aladdin Chemistry Co., Ltd. and purified by vacuum distillation prior to use. Styryphenol poloxyethylene ether (600#A), sodium dodecyl sulfate (SDS), octylphenol polyoxyethylene ether (NP-10), and sodium bicarbonate were purchased from Aladdin Chemistry Co., Ltd. and used as received. Potassium peroxydisulfate (KPS) purchased from Aladdin Chemistry Co., Ltd. was recrystallized from deionized water (40°C) prior to use. 2,2,2-Trifluoroethyl methacrylate (MF3) and dodecafluoroheptyl methacrylate (MF12) were kindly supplied by Dalian Zhenbang Fluorocarbon Paint Stock Co., Ltd.

Table 1: Recipes for polyacrylate emulsion latex.

Sample	CTFE (g)	VAc (g)	BA (g)	Veova (g)	MF3 (g)	MF12 (g)	Water (g)
WS1	80	85	40	40	0	0	600
WS2	80	25	40	40	60	0	600
WS3	80	25	40	40	0	60	600

2.2. Synthesis of Fluorinated Polyacrylate Latexes. The fluorine polyacrylate latexes were prepared by semicontinuous emulsion polymerization, using emulsifier mixtures containing 600#A, SDS, and NP-10 (at a weight ratio of 5 : 4 : 1). The recipes were described in Table 1. Typically, a preemulsion of 80 wt% emulsifier mixtures, all monomers except for CTFE, and 35 wt% distilled water were mixed in the beaker and stirred vigorously for 30 min at room temperature according to the recipes. All initiators (KPS) were added in the beaker containing 30 wt% distilled water and then stirred for 30 min at room temperature, which lastly formed initiator solution.

A 1 L autoclave equipped with a reflux condenser, a thermometer, and a mechanical stirrer was filled with a mixture of 20 wt% emulsifier mixtures, the rest 35 wt% distilled water, and 0.9 g dicarbonate in nitrogen atmosphere. The mixture was first stirred for 30 min. Then, the 8 wt% resultant preemulsion and all the CTFE were both added into the autoclave with an appropriate dropping rate at room temperature. When the 8 wt% resultant preemulsion and CTFE were completely fed, the temperature was then increased to 60°C. Simultaneously, the 92 wt% resultant preemulsion and the resultant initiator solution were both added dropwise into the autoclave, which lasted for 3 h. In fact, we use gravimetric analysis to calculate the conversion rate [39, 40]. Briefly, 2 g of emulsion was cast onto a weighing disk, quenched with hydroquinone, and then dried to the constant weight at 120°C. After that, the reaction was carried out continuously for another 3 h.

2.3. Preparation of Latex Film. The films were prepared by casting the resultant emulsion latexes onto cleaned glass plates and dried at room temperature for 2 days. After that, the films were allowed to transfer to a vacuum oven and further dried for additional 24 h.

2.4. Characterization. To observe the storage stability of the fluorinated emulsions, all of the emulsions prepared were stored at room temperature for more than 1 year under the sealed state. The viscosity of the emulsion was measured with a numerical viscometer (NBJ-8S, Shanghai Jitai Co., Ltd.). The particle size and zeta potential (ζ) of the dispersions were measured by a Malvern Zetasizer Nano-ZS90 instrument at room temperature. Contact angles of water were tested by a contact angle goniometer at room temperature. A FTIR spectrum (Nicolet 20XB) was performed to characterize the freeze-dried nanoparticles. Thermal gravimetric analysis (TGA) measurements were performed on a NETZSCH TG 209 thermal analyzer. X-ray photoelectron spectroscopy (XPS) analyses for surface of latex films were performed on a Perkin Elmer ESCA 5600 spectrometer with a MgKα X-ray source (1253.6 eV). Refractive index was measured by an α-SE Woollam spectroscopic ellipsometer.

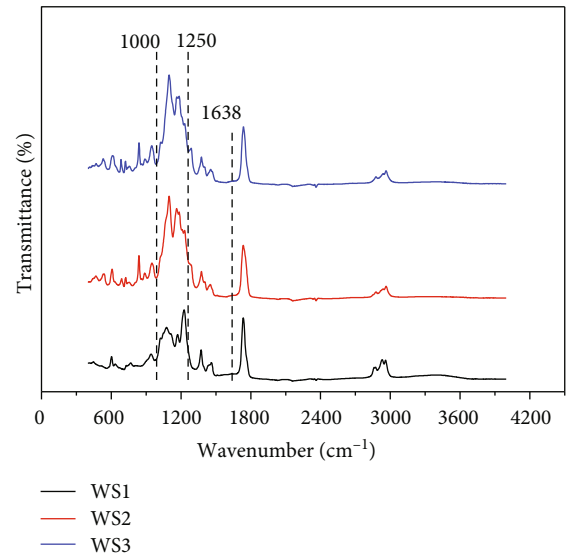

Figure 1: FTIR spectra of the emulsion latex.

To evaluate the size and morphology of polyacrylate nanoparticles, one drop of the nanoparticle suspension was diluted in 10 mL of water and 40 μL of this solution were deposited on a copper grid (400 mesh) previously covered with an 8 nm thick carbon layer. After 30 s, the droplet was removed and images of the slices were taken with a JEM-2100 Plus transmission electron microscope. The morphology and microstructure of the latex films were characterized using a JEOL JSM-7800F scanning electron microscope (SEM).

Water absorption tests were performed as described below. Briefly, samples were dried at 100°C and then cooled down to ambient temperature. The sample was weighed as w_0. After that, we immerse the samples in deionized water for 24 h. w represents the weight of the sample after immersed. Water absorption (w%) was defined as follows:

$$w\% = \frac{w - w_0}{w_0}. \quad (1)$$

3. Results and Discussion

3.1. Polyacrylate Nanoparticle Chemical Structure Characterization. The latex nanoparticles with different contents of fluorine were synthesized by semicontinuous emulsion polymerization. Three systems (Table 1) were synthesized: WS1 (without fluorinate acrylate), WS2 (containing 2,2,2-trifluoroethyl methacrylate (MF3)), and WS3 (containing dodecafluoroheptyl methacrylate (MF12)). The solid contents of WS1, WS2, and WS3 were 30.2%, 31.5%, and 30.5%, respectively. The coagulation ratio of WS1, WS2, and WS3 was 1%, 2.6%, and 3.5%, respectively. FTIR and XPS were used to determine the chemical structures and fluorine content of fluorinated latex nanoparticles.

FTIR spectra of samples are shown in Figure 1. The inexistence of C=C peak at 1638 cm^{-1} for all samples demonstrates that all monomers have been successfully

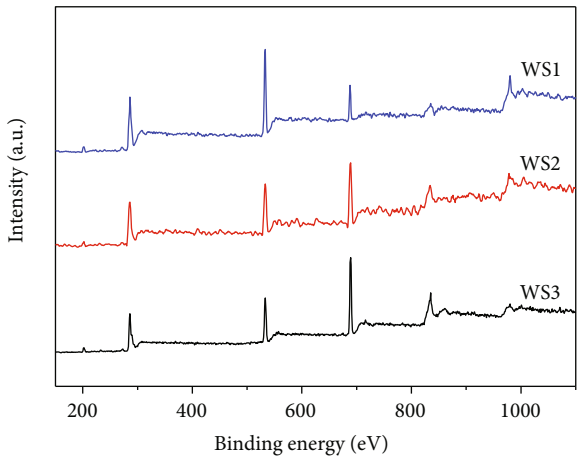

Figure 2: Wide-scan XPS spectra for latex emulsion.

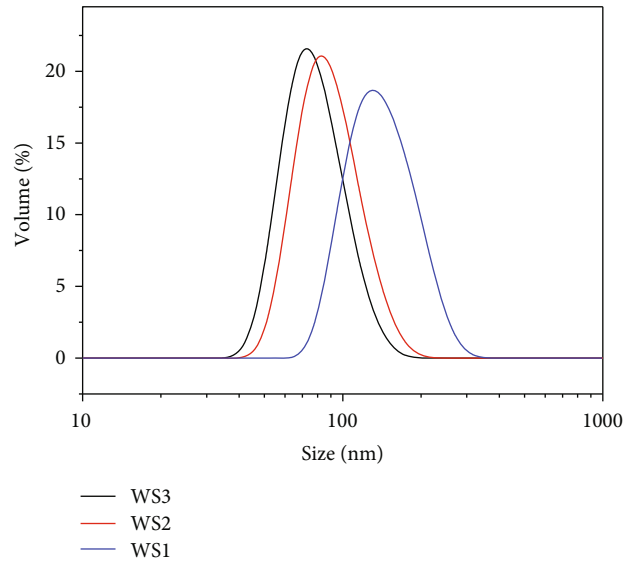

Figure 3: Particle size and distribution of latexes with different fluorine contents.

incorporated in the polymer chain. In comparison with the WS1, the band absorptions of WS2 and WS3 in the range from 1000 to 1250 cm^{-1} become broadened and enhanced obviously. All of these broad bands could be related to the C-F complex vibration absorption peaks. In contrast, for WS1, relative to WS2 and WS3, the $-CH_2-$ absorption becomes stronger. The FTIR results indicate that more fluorinated groups have been incorporated into the polymer chain of WS2 and WS3.

The XPS survey spectra for the polymer films recorded at the take-off angle of 0° are shown in Figure 2. The signals at 687, 534, 283, and 200 eV are assigned to the fluorine, oxygen, carbon, and chlorine, respectively. The content of fluorine could be examined based on the peak area of the 687 eV peak. Compared with WS1, WS2 and WS3 have stronger fluorine peak and weaker carbon and oxygen peak. XPS results indicate that more fluorine has been introduced into the polymer chain for WS2 and WS3. The FTIR and XPS results reveal successful preparation of high fluorine content of latex nanoparticles by semicontinuous emulsion polymerization.

3.2. Effects of Fluorine Contents on Stability of Nanoparticles. Many factors, such as pH, crystallinity, and particle size, can affect the stability of polymeric nanoparticles in water [12, 32]. Moreover, in this paper, all nanoparticles were obtained by random copolymerization, so there is no crystallization, and the pH of the emulsion system is 7. Figure 3 shows the particle size curves of different nanoparticles. It is seen that the curve of WS1 is to the right of WS2 and WS3. The average particle sizes of WS1, WS2, and WS3 are 143.5, 97.3, and 93.3 nm, respectively. This indicates that nanoparticles with higher fluorine content have smaller particle sizes, and adjusting the fluorine content can effectively adjust the size of nanoparticles. The same phenomenon was observed from some other papers [41, 42]. We deduce that during the polymerization of the WS2 or WS3 sample, the hydrophobic fluorine monomer and the hydrophilic CTFE component are copolymerized into the polymer backbone to form a surfactant-like amphiphilic polymer. Attributed to the self-emulsification for generated amphiphilic polymer, it can keep the micelles stable and prevent themselves from stealing the emulsifiers of other micelles at the nucleation process, which in turn increases the number of micelles. The presence of more micelles can provide more nucleation sites for the nanoparticles, resulting in smaller particle sizes and narrower size distribution [43–45]. Additionally, creaming velocity (v_{Stokes}) which can evaluate the long-term stability of nanoparticles is described using the Stokes terminal velocity equation [13].

$$v_{Stokes} = \frac{d_p^2 |\rho - \rho_0| g}{18 \mu_c}, \quad (2)$$

where d_p is the diameter of emulsion particle, p and p_0 are the density of the water and the emulsion, u_c is the viscosity of water, and g is the gravity acceleration velocity. Obviously, in the emulsion system, the diameter of the emulsion particle has a significant effect on the creaming velocity. In addition, the viscosity and the density of the emulsion are similar (Table 2). That is, the smaller the particle, the slower the creaming velocity. The long-term storage stability of the fluorinated emulsions was compared after 1 year (Figure 4). The sample WS1 with a larger particle size was very unstable, as a clearly creaming was observed after 1 year. A better stabilization of the sample WS2 (Figure 4) and WS3 (Figure S1 in the supporting information) was observed. The cause of this phenomenon is that the high hydrophobicity of fluorinated monomers compared with ordinary monomers leads to weak mobility in water. So the failure of micelles to obtain enough fluorinated monomers causes the smaller size of latex particles in emulsion polymerization [46]. Besides, WS1 has a larger particle dispersibility index (PDI) than WS2 and WS3 (Table 2), which represents a broader particle size distribution for WS1. This agrees with the result of TEM images for different polyacrylate nanoparticles (Figure S2 in the supporting information).

Table 2: Viscosity, density, appearance, size, PDI, zeta potential, and conversion of the latexes.

Sample	Viscosity (mPa·s)	Density (g/mL)	Appearance	Dispersion size (nm)	PDI	Zeta potential (mV)	Conversion (%)
WS2	14	1.104	Milkiness blue	97.3	0.02	-40.2	**97.62**
WS3	16	1.169	Milkiness blue	93.3	0.052	-53	**95.8**
WS1	18.5	1.053	Grey blue	143.5	0.073	-61.6	**98.3**

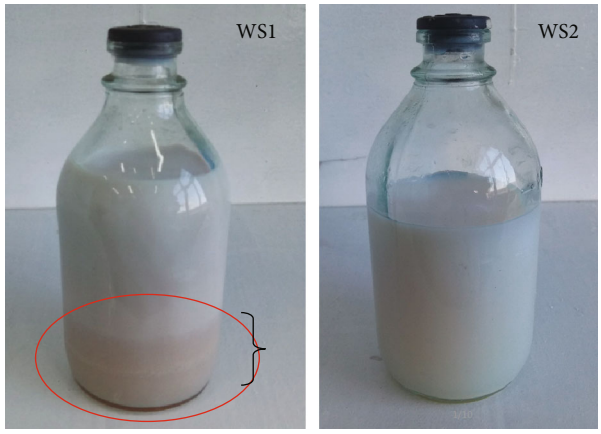

Figure 4: Visual observations of the latexes with different fluorine contents after 1 year.

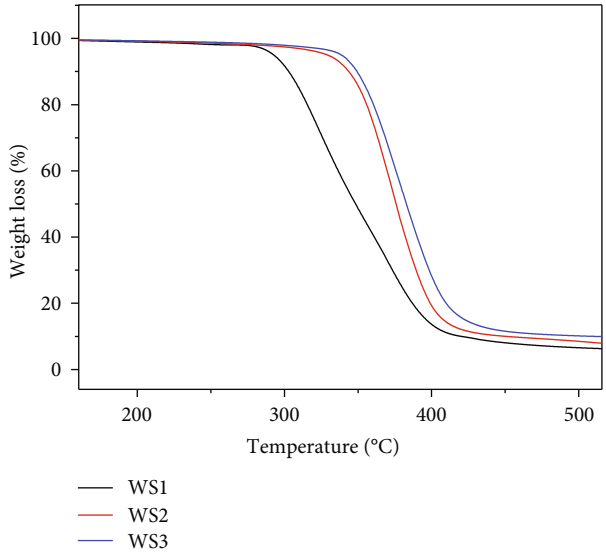

Figure 5: TGA curves of the latex films with different fluorine contents.

With regard to WS1, it is strongly influenced by internal hydrophilic components and nanoparticles present swelling behavior when distributed in aqueous solution. Along with water volatilization during sample preparation, the microspheres of WS1 are more likely to undergo obvious deformation and the particle size is substantially greater than 100 nm. By contrast, due to the presence of fluorine components, WS2 and WS3 show limited water absorption, thus maintaining basically microsphere shape and smaller particle size (less than 100 nm). In macroscopic view, particles with a certain range may exhibit different colors.

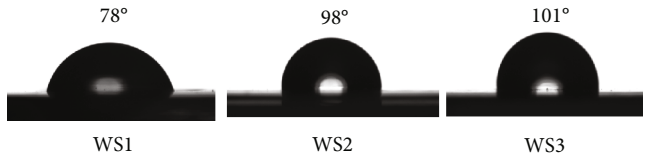

Figure 6: Water contact angles of the latex films with different fluorine contents.

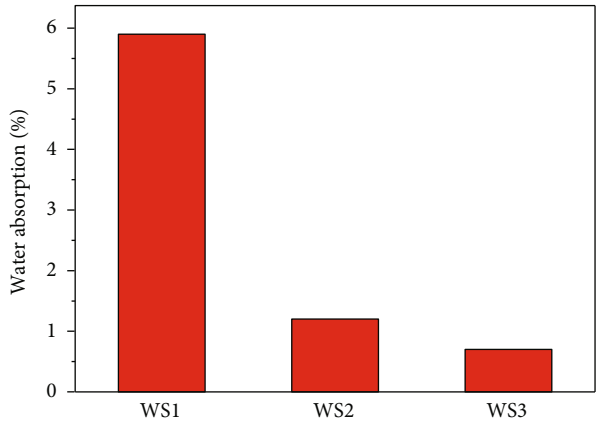

Figure 7: Water absorptions of the latex films with different fluorine contents.

For similar particle size difference of WS2 and WS3, their appearance is basically the same. It is known that latex particles with smaller size have better stability. Accompanied by a long-time placement, the unfavorable impact of larger size and wider PDI are more significant, namely, WS1 takes on obvious stratification. Accordingly, higher fluorine contents could improve the stability of latex particles. In fact, the surface charge of nanoparticles would affect their stability in water. On the other hand, its chemical composition can alter the nanoparticle charge [30]. Research shows that the zeta potential of WS1, WS2, and WS3 is -40.2 mV, -53 mV, and -61.6 mV, respectively. Higher zeta potential values represent more stable storage [47, 48]. The specific reason may be that the C-F bond of MF3 or MF12 was introduced into the nanoparticles, reducing their hydrophilicity. Hence, the nanoparticles are inclined to absorb specific ion rather than water, making the surface potentials higher [49, 50]. By calculation, the conversion of WS1, WS2, and WS3 is 97.62%, 95.8%, and 98.3%, respectively.

3.3. Thermal and Hydrophobic Properties of Latex Films Prepared with Different Fluorine Contents. The TGA curves as the function of temperature are illustrated in Figure 5. It

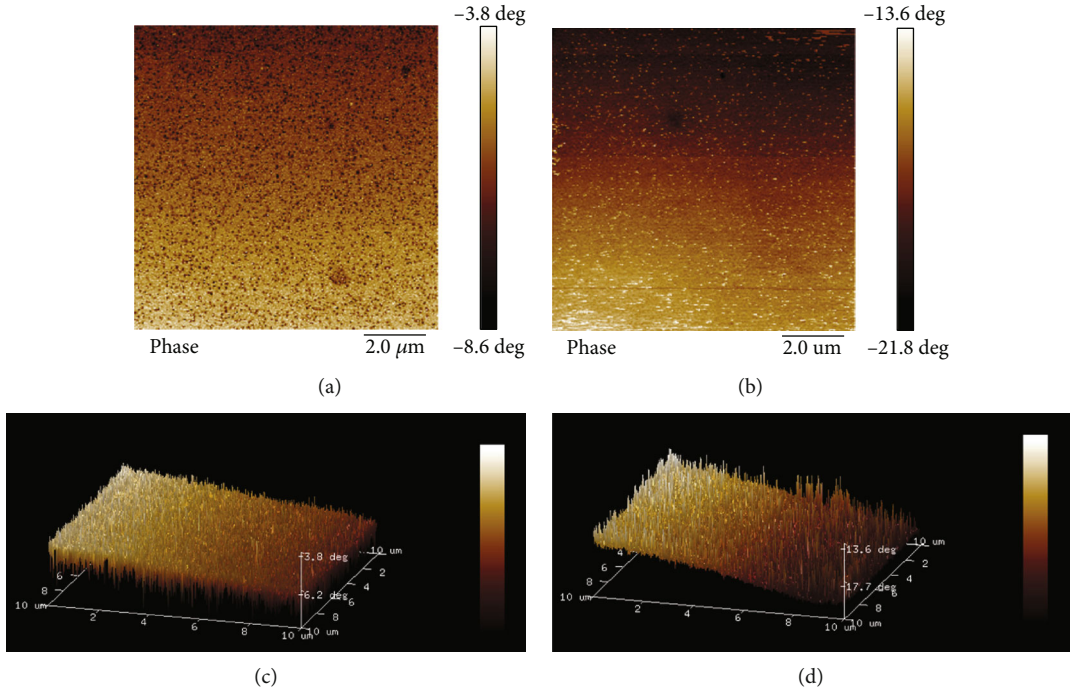

Figure 8: AFM phase images of the films for (a) WS1 and (b) WS3. AFM three-dimensional height images of the films for (c) WS1 and (d) WS3.

can be seen from Figure 5 that the initial decomposition (5% weight loss) temperature of WS3 is 338°C, which is 9°C higher than that of WS2 and 46°C higher than that of WS1. It is also found that the temperature of the 5% weight loss of latex films slightly increases with the increase of fluorine contents. The similar phenomenon has also been observed for the other weight loss of latex films with different fluorine contents. The reason is contributed to that the cleavage temperature of the pendant fluorine side groups is higher than that of the poly(vinyl acetate) chain. Thus, the thermal stability of films is significantly improved due to the introducing of more fluorine in the particles.

The surface hydrophobicity of the latex films with varied fluorine contents was investigated by the measurements of water contact angle (Figure 6). For the WS1, the water contact angle is only 76°. With the introduction of more fluorine, the water contact angle increased rapidly to 98° and 101° for the sample of WS2 and WS3. Therefore, for this series of latex films, a highly hydrophobic surface can be obtained by successful incorporating of more fluorine into the polymer. As for the copolymerized monomers MF3 and MF12, they contain a low surface tension of $-CF_3$ (6 mN/m), $-CF_2H$ (15 mN/m), and $-CF_2-CF_2-$ (18.5 mN/m) groups [51, 52]. When the VAc dominated by -CH3 (24 mN/m) was replaced, the contact angle was significantly smaller according to the one-liquid method formula. In addition, as shown in Figure 7, with the increase of fluorine contents, the hydrophobicity of the bulk latex films increases while the films' water absorptions reduce. As can be seen, for WS2 and WS3, water absorption is at a relatively low level due to the hydrophobic fluorinated moieties at the surface, which prevents water from entering into the bulk of materials. And the water absorptions of SW1, SW2, and SW3 are 5.9%, 1.2%, and 0.7%, respectively. Water absorption is actually a manifestation of wettability [53]. If the film surface has plenty of hydrophilic groups, it is advantageous for the water to enter the polymer film body under the action of capillary absorption through the liquid-solid surface pores. To the contrary, the hydrophobic C-F bond blocks the entry of water molecules and reduces their wettability [54]. It is believed that more fluorine can endow the films with greater water repellency.

3.4. Effect of Fluorine Contents on Surface Morphology and Refractive Index of Latex Films. The variations in the surface morphologies caused by fluorine contents were examined by atomic force microscopy (AFM). Since SEM acquires only two-dimensional images, it cannot exhibit the roughness information of the film [53]. SEM images of different polyacrylate latex films in Figure S3 are similar. The evolution of phase images of the films with the increase of fluorine content is depicted in Figures 8(a) and 8(b). The previous studies on fluorinated aliphatic polyesters or polyacrylates have showed that the fluorinated moieties are stiffer and harder, so look as the brighter regions at the higher phase angle. On the contrary, the aliphatic polyacrylate or polyester segments are relatively flexible and soft, related to the dark part. As can be seen from the phase images, the phase images exhibit more bright domains, indicating the aggregation of fluorinated groups is on the surface. The three-dimensional images of latex films are shown in Figures 8(c) and 8(d). The roughness is influenced greatly by the amount of fluorine contents. The surface of sample WS1 is very smooth. In comparison, the surface of sample WS3 has a large number of "pointed bumps," which corresponds to bright points in the phase images, making

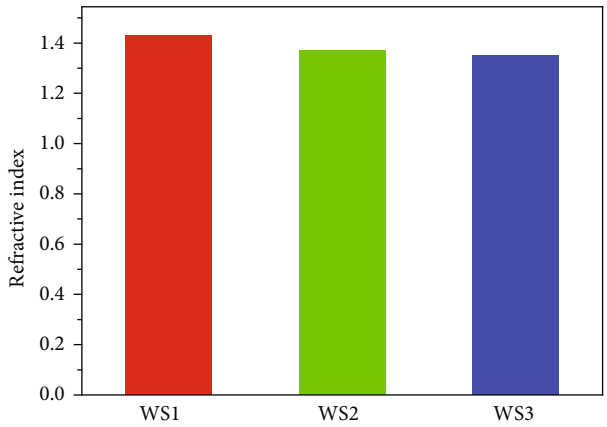

Figure 9: Variations of refractive index values with the fluorine content for the polymer films.

the membrane surface rough. This result is consistent with the data of contact angle. Because the rough surface of sample can improve the hydrophobicity of film. The refractive index of latex films is shown in Figure 9. The refractive index for WS3, WS2, and WS1 is 1.35, 1.37, and 1.43, respectively. With the copolymerizing of more fluorinated moieties, the refractive index of films decreases. Because it is well known that the replacement of aliphatic C-H bonds with elements of higher masses such as C-F groups substantially lowers the energy of the fundamental bond vibration modes and greatly decreases the optical absorption at light wavelengths.

4. Conclusions

The series of polyacrylate nanoparticles were successfully synthesized by semicontinuous emulsion polymerization. The chemical structures of the polymers were confirmed by FTIR and XPS. The DLS curves show that the WS2 and WS3 have smaller size of nanoparticles, meaning more fluorine contents can decrease the size of nanoparticles. Compared to nanoparticles with lower fluorine contents, nanoparticles with higher fluorine contents are more stable owing to smaller size. In addition, more fluorinated moieties incorporated into latex films lead to better hydrophobic properties, higher thermal stability, and lower refractive index. The combination of the above excellent properties endows the high fluorinated polymers with promising applications in the fabrication of functional devices.

Data Availability

All the data used to support the findings of this study are available and have been included within the article. The authors give permission for publisher and readers to access all data related to the findings in this article.

Conflicts of Interest

The authors declare that they have no conflict of interest.

Authors' Contributions

Hongzhu Liu and Gaofan Zhang contributed equally to this work.

Acknowledgments

This work was financially supported by the Project of New Seedling Talents Program of Zhejiang Province (No. 2018R434004), the General Research Projects of Zhejiang Provincial Department of Education (No. Y201840153), and Key R&D Projects of Lishui Science and Technology Bureau (No. 2016ZDYF10).

Supplementary Materials

Figure S1: visual observation for WS3 after 1 year. Figure S2: TEM images of different polyacrylate nanoparticles from (a) WS1, (b) WS2, and (c) WS3. Figure S3: SEM images of different polyacrylate latex films from (a) WS1, (b) WS2, and (c) WS3. *(Supplementary Materials)*

References

[1] M. Elsabahy and K. L. Wooley, "Design of polymeric nanoparticles for biomedical delivery applications," *Chemical Society Reviews*, vol. 41, no. 7, pp. 2545–2561, 2012.

[2] S. Lin, T. Li, P. Xie et al., "Targeted delivery of doxorubicin to tumour tissues by a novel legumain sensitive polygonal nanogel," *Nanoscale*, vol. 8, no. 43, pp. 18400–18411, 2016.

[3] L. M. Ensign, R. Cone, and J. Hanes, "Oral drug delivery with polymeric nanoparticles: the gastrointestinal mucus barriers," *Advanced Drug Delivery Reviews*, vol. 64, no. 6, pp. 557–570, 2012.

[4] L. Han, Y. Shu, X. Wang, X. Chen, and J. Wang, "Encapsulation of silica nano-spheres with polymerized ionic liquid for selective isolation of acidic proteins," *Analytical and Bioanalytical Chemistry*, vol. 405, no. 27, pp. 8799–8806, 2013.

[5] M. M. Yallapu, N. Chauhan, S. F. Othman et al., "Implications of protein corona on physico-chemical and biological properties of magnetic nanoparticles," *Biomaterials*, vol. 46, pp. 1–12, 2015.

[6] Q. Sun, Z. Dai, X. Meng, and F.-S. Xiao, "Porous polymer catalysts with hierarchical structures," *Chemical Society Reviews*, vol. 44, no. 17, pp. 6018–6034, 2015.

[7] W. Zhang, Y. Sun, and L. Zhang, "In situ synthesis of monodisperse silver nanoparticles on sulfhydryl-functionalized poly(glycidyl methacrylate) microspheres for catalytic reduction of 4-nitrophenol," *Industrial & Engineering Chemistry Research*, vol. 54, no. 25, pp. 6480–6488, 2015.

[8] A. Galperin, D. Margel, J. Baniel, G. Dank, H. Biton, and S. Margel, "Radiopaque iodinated polymeric nanoparticles for X-ray imaging applications," *Biomaterials*, vol. 28, no. 30, pp. 4461–4468, 2007.

[9] X. Wang, M. Tu, K. Yan et al., "Trifunctional polymeric nanocomposites incorporated with Fe_3O_4/iodine-containing rare earth complex for computed X-ray tomography, magnetic resonance, and optical imaging," *ACS Applied Materials & Interfaces*, vol. 7, no. 44, pp. 24523–24532, 2015.

[10] W. Tungittiplakorn, L. W. Lion, C. Cohen, and J. Y. Kim, "Engineered polymeric nanoparticles for soil remediation,"

Environmental Science & Technology, vol. 38, no. 5, pp. 1605–1610, 2004.

[11] Z. Wang, W. Ye, X. Luo, and Z. Wang, "Heat-resistant crack-free superhydrophobic polydivinylbenzene colloidal films," *Langmuir*, vol. 32, no. 12, pp. 3079–3084, 2016.

[12] M. L. T. Zweers, D. W. Grijpma, G. H. M. Engbers, and J. Feijen, "The preparation of monodisperse biodegradable polyester nanoparticles with a controlled size," *Journal of Biomedical Materials Research: Part B Applied Biomaterials*, vol. 66B, no. 2, pp. 559–566, 2003.

[13] C. Chinwanitcharoen, S. Kanoh, T. Yamada, S. Hayashi, and S. Sugano, "Preparation of aqueous dispersible polyurethane: effect of acetone on the particle size and storage stability of polyurethane emulsion," *Journal of Applied Polymer Science*, vol. 91, no. 6, pp. 3455–3461, 2004.

[14] Z. Geng, M. Huo, J. Mu et al., "Ultra low dielectric constant soluble polyhedral oligomeric silsesquioxane (POSS)-poly(aryl ether ketone) nanocomposites with excellent thermal and mechanical properties," *Journal of Materials Chemistry C*, vol. 2, no. 6, pp. 1094–1103, 2014.

[15] H. Kaur, M. Ahuja, S. Kumar, and N. Dilbaghi, "Carboxymethyl tamarind kernel polysaccharide nanoparticles for ophthalmic drug delivery," *International Journal of Biological Macromolecules*, vol. 50, no. 3, pp. 833–839, 2012.

[16] Y. Bao, J. Ma, X. Zhang, and C. Shi, "Recent advances in the modification of polyacrylate latexes," *Journal of Materials Science*, vol. 50, no. 21, pp. 6839–6863, 2015.

[17] Y. Sun, X. Zhao, R. Liu, G. Chen, and X. Zhou, "Synthesis and characterization of fluorinated polyacrylate as water and oil repellent and soil release finishing agent for polyester fabric," *Progress in Organic Coatings*, vol. 123, pp. 306–313, 2018.

[18] J. Zhou, Y. Cui, L. Wang, J. Ma, and P. Wei, "Synthesis of nano-TiO_2/fluorinated polyacrylate core-shell latex and its application in fabric finishing," *Polymer Composites*, vol. 39, no. 12, pp. 4467–4476, 2018.

[19] Y. Xie, W. Liu, L. Liang et al., "Enhancement of anticorrosion property and hydrophobicity of modified epoxy coatings with fluorinated polyacrylate," *Colloids and Surfaces A: Physicochemical and Engineering Aspects*, vol. 579, article 123659, 2019.

[20] Y. Yang, T. Zhang, J. Yan et al., "Preparation and photochromic behavior of spiropyran-containing fluorinated polyacrylate hydrophobic coatings," *Langmuir*, vol. 34, no. 51, pp. 15812–15819, 2018.

[21] Y. Huang, Y. Pan, W. Wang, L. Jiang, and Y. Dan, "Synthesis and properties of partially biodegradable fluorinated polyacrylate: poly(*l*-lactide)-*co*-poly(hexafluorobutyl acrylate) copolymer," *Materials & Design*, vol. 162, pp. 285–292, 2019.

[22] Y. Bao, C. Feng, C. Wang, J. Ma, and C. Tian, "Hygienic, antibacterial, UV-shielding performance of polyacrylate/ZnO composite coatings on a leather matrix," *Colloids and Surfaces A: Physicochemical and Engineering Aspects*, vol. 518, pp. 232–240, 2017.

[23] K. Hadinoto, P. Phanapavudhikul, Z. Kewu, and R. B. H. Tan, "Dry powder aerosol delivery of large hollow nanoparticulate aggregates as prospective carriers of nanoparticulate drugs: effects of phospholipids," *International Journal of Pharmaceutics*, vol. 333, no. 1-2, pp. 187–198, 2007.

[24] E. R. Brandt, K. S. Sriprakash, R. I. Hobb et al., "New multideterminant strategy for a group A streptococcal vaccine designed for the Australian Aboriginal population," *Nature Medicine*, vol. 6, no. 4, pp. 455–459, 2000.

[25] C. Y. Ang, S. Y. Tan, X. Wang et al., "Supramolecular nanoparticle carriers self-assembled from cyclodextrin- and adamantane-functionalized polyacrylates for tumor-targeted drug delivery," *Journal of Materials Chemistry B*, vol. 2, no. 13, pp. 1879–1890, 2014.

[26] P. Chen, Z. Cheng, F. Chu, Y. Xu, and C. Wang, "Fabrication of polyacrylate core-shell nanoparticles via spray drying method," *Journal of Nanoparticle Research*, vol. 18, no. 5, 2016.

[27] S. C. Abeylath and E. Turos, "Glycosylated polyacrylate nanoparticles by emulsion polymerization," *Carbohydrate Polymers*, vol. 70, no. 1, pp. 32–37, 2007.

[28] H. Wang, Y. Niu, G. Fei, Y. Shen, and J. Lan, "In-situ polymerization, rheology, morphology and properties of stable alkoxysilane-functionalized poly (urethane-acrylate) microemulsion," *Progress in Organic Coatings*, vol. 99, pp. 400–411, 2016.

[29] S. Aben, C. Holtze, T. Tadros, and P. Schurtenberger, "Rheological investigations on the creaming of depletion-flocculated emulsions," *Langmuir*, vol. 28, no. 21, pp. 7967–7975, 2012.

[30] B. P. Binks and C. P. Whitby, "Nanoparticle silica-stabilised oil-in-water emulsions: improving emulsion stability," *Colloids and Surfaces A: Physicochemical and Engineering Aspects*, vol. 253, no. 1-3, pp. 105–115, 2005.

[31] S. Lazzari, D. Moscatelli, F. Codari, M. Salmona, M. Morbidelli, and L. Diomede, "Colloidal stability of polymeric nanoparticles in biological fluids," *Journal of Nanoparticle Research*, vol. 14, no. 6, 2012.

[32] D. Lemoine, C. Francois, F. Kedzierewicz, V. Preat, M. Hoffman, and P. Maincent, "Stability study of nanoparticles of poly(ε-caprolactone), poly(d,l-lactide) and poly(d,l-lactide-co-glycolide)," *Biomaterials*, vol. 17, no. 22, pp. 2191–2197, 1996.

[33] J. Logie, S. C. Owen, C. K. McLaughlin, and M. S. Shoichet, "PEG-graft density controls polymeric nanoparticle micelle stability," *Chemistry of Materials*, vol. 26, no. 9, pp. 2847–2855, 2014.

[34] J. Yang, Y. Zhu, J. Zhu et al., "Influences of maleic reactive surfactants with different EO chain lengths on the properties of the acrylate latices," *Journal of Coatings Technology and Research*, vol. 12, no. 6, pp. 1041–1052, 2015.

[35] Z. Zhang, W. Shen, J. Ling, Y. Yan, J. Hu, and Y. Cheng, "The fluorination effect of fluoroamphiphiles in cytosolic protein delivery," *Nature Communications*, vol. 9, no. 1, 2018.

[36] W. Yao, Y. Li, and X. Huang, "Fluorinated poly(meth)acrylate: synthesis and properties," *Polymer*, vol. 55, no. 24, pp. 6197–6211, 2014.

[37] H. Mei and F. Ibrahim, "Two new diazonium bis(perfluoroalkyl)arylsulfonyl imide zwitterionic monomers from perfluoro(3-oxa-4-pentene)sulfonyl fluoride for proton exchange membrane fuel cells," *Journal of Fluorine Chemistry*, vol. 199, pp. 46–51, 2017.

[38] H. Li, L. Wang, M. Wang et al., "Engineered multifunctional fluorinated film based on semicontinuous emulsion polymerization using polymerizable quaternary ammonium emulsifiers," *International Journal of Polymer Science*, vol. 2018, Article ID 5659137, 9 pages, 2018.

[39] W. Xu, Q. An, L. Hao, Z. Sun, and W. Zhao, "Synthesis and properties of cationic fluorinated polyacrylate soap-free latex,"

Journal of Macromolecular Science, Part A: Pure and Applied Chemistry, vol. 50, no. 6, pp. 670–677, 2013.

[40] J. Zhou, X. Chen, H. Duan, and J. Ma, "Fluorosilicone modified polyacrylate emulsifier-free latex: synthesis, properties, and application in fabric finishing," *Fibers and Polymers*, vol. 18, no. 4, pp. 625–632, 2017.

[41] K. Landfester, R. Rothe, and M. Antonietti, "Convenient synthesis of fluorinated latexes and core–shell structures by miniemulsion polymerization," *Macromolecules*, vol. 35, no. 5, pp. 1658–1662, 2002.

[42] R. F. Linemann, T. E. Malner, R. Brandsch, G. Bar, W. Ritter, and R. Mülhaupt, "Latex blends of fluorinated and fluorine-free acrylates: emulsion polymerization and tapping mode atomic force microscopy of film formation," *Macromolecules*, vol. 32, no. 6, pp. 1715–1721, 1999.

[43] T. F. Mccarthy, R. Williams, J. F. Bitay, K. Zero, M. S. Yang, and F. Mares, "Surfactant-free emulsion polymerization of chlorotrifluoroethylene with vinylacetate or vinylidene fluoride," *Journal of Applied Polymer Science*, vol. 70, no. 11, pp. 2211–2225, 1998.

[44] Q. Zhang, X. Zhan, and F. Chen, "Miniemulsion polymerization of a fluorinated acrylate copolymer: kinetic studies and nanolatex morphology characterization," *Journal of Applied Polymer Science*, vol. 104, no. 1, pp. 641–647, 2007.

[45] D. Missirlis, R. Kawamura, N. Tirelli, and J. A. Hubbell, "Doxorubicin encapsulation and diffusional release from stable, polymeric, hydrogel nanoparticles," *European Journal of Pharmaceutical Sciences*, vol. 29, no. 2, pp. 120–129, 2006.

[46] Y. Cheng and Z. Wang, "Fluorinated poly(isobornyl methacrylate–co–butyl acrylate) core–shell latex nanoparticles: synthesis, morphology and wettability of films," *Polymer*, vol. 54, no. 12, pp. 3047–3054, 2013.

[47] W. Abdelwahed, G. Degobert, S. Stainmesse, and H. Fessi, "Freeze-drying of nanoparticles: formulation, process and storage considerations," *Advanced Drug Delivery Reviews*, vol. 58, no. 15, pp. 1688–1713, 2006.

[48] F. Gambinossi, S. E. Mylon, and J. K. Ferri, "Aggregation kinetics and colloidal stability of functionalized nanoparticles," *Advances in Colloid and Interface Science*, vol. 222, pp. 332–349, 2015.

[49] G. Li, Y. Shen, and Q. Ren, "Effect of fluorinated acrylate on the surface properties of cationic fluorinated polyurethane-acrylate hybrid dispersions," *Journal of Applied Polymer Science*, vol. 97, no. 6, pp. 2192–2196, 2005.

[50] A. Fahami, G. W. Beall, and T. Betancourt, "Synthesis, bioactivity and zeta potential investigations of chlorine and fluorine substituted hydroxyapatite," *Materials Science and Engineering: C*, vol. 59, pp. 78–85, 2016.

[51] E. G. Shafrin and W. A. Zisman, "Constitutive relations in the wetting of low energy surfaces and the theory of the retraction method of preparing monolayers," *The Journal of Physical Chemistry*, vol. 64, no. 5, pp. 519–524, 1960.

[52] M. K. Bernett and W. A. Zisman, "Wetting properties of acrylic and methacrylic polymers containing fluorinated side chain," *The Journal of Physical Chemistry*, vol. 66, no. 6, pp. 1207-1208, 1962.

[53] Z. Wang and Z. Wang, "Synthesis of cross-linkable fluorinated core–shell latex nanoparticles and the hydrophobic stability of films," *Polymer*, vol. 74, pp. 216–223, 2015.

[54] G. Alessandrini, M. Aglietto, V. Castelvetro, F. Ciardelli, R. Peruzzi, and L. Toniolo, "Comparative evaluation of fluorinated and unfluorinated acrylic copolymers as water-repellent coating materials for stone," *Journal of Applied Polymer Science*, vol. 76, no. 6, pp. 962–977, 2000.